Technological Applied Sciences Status : Research Article
ISSN: 1308 7258 Received: 13.10.2025
Article ID: 2A0214 Accepted: 26.04.2026

Feyzanur Ozden
Erzincan Binali Yildirim University, feyzanur.ozden@ogr.ebyu.edu.tr, Erzincan-Türkiye
Canan Tastimur
Erzincan Binali Yildirim University, ctastimur@erzincan.edu.tr, Erzincan-Türkiye

DOI	http://dx.doi.org/10.12739/NWSA.2026.21.2.2A0214	
ORCID ID	0009-0002-9157-5821	0000-0002-3714-6826
Corresponding Author	Canan Taştimur	

A NOVEL APPROACH TO INDUSTRIAL FABRIC DEFECT ANALYSIS USING ADAPTIVE ANOMALY REASONING AND HIERARCHICAL FEATURE LEARNING

ABSTRACT

One of the most significant problems businesses face in their production processes is the accurate and rapid detection of defective areas on the product surface. In this study, defect detection and classification were performed on our fabric defect dataset containing one normal and four defective fabric samples. Transformer-based unsupervised fault detection and CNN-transformer-based supervised fault classification are designed as an integrated architecture. During fault detection, images are separated into patch-based features, and then contextual relationships are learned via the transformer. In fault detection, our innovative module creates a memory bank with normal fabric images, and faulty regions in the fabric are detected thanks to the Mahalanobis distance and statistical distribution deviations. In the fault classification phase, Channel Attention, with the CNN-transformer hybrid structure, achieved a test accuracy of 97.78%. In addition, the model's attention mechanism, which correctly directs attention to faulty areas, is presented with visual results.

Keywords: Adaptive Feature Fusion, Anomaly Localization, Contextual Representation Learning, Explainable Artificial İntelligence, Industrial Defect Inspection

1. INTRODUCTION

The digital transformation currently underway in the manufacturing sector necessitates making quality control processes faster, more reliable, and automated. Especially with the widespread adoption of smart manufacturing systems, early detection of defects on production lines is crucial for both reducing production costs and improving product quality. In this context, accurately identifying surface defects stands out as one of the most critical stages of quality control processes. Surface defects, commonly encountered in the textile industry, are a significant factor directly affecting product performance and customer satisfaction. Traditional quality control methods are largely based on human observation, making them both time-consuming and prone to errors. In modern production lines with increased production speeds, the inadequacy of manual inspection methods is clear. This situation has made the development of automated and intelligent systems inevitable. At this point, deep learning-based methods, thanks to their successes in image processing, offer a significant alternative in solving the surface defect detection problem. However, the variety of different defect types and the complexity of datasets make it difficult for a single model to demonstrate sufficient performance.

How to Cite:
Özden, F. and Taştimur, C., (2026). A novel approach to industrial fabric defect analysis using adaptive anomaly reasoning and hierarchical feature learning. Technological Applied Sciences, 21(2):17-29, DOI: 10.12739/NWSA.2026.21.2.2A0214.

This study aims to develop high-performance deep learning models for the early detection of defects on the product surface in intelligent manufacturing systems. Early detection of defects in production processes reduces costs and improves product quality. The increasing importance of quality control processes and the use of autonomous systems for product defect diagnosis have increased the demand for research in this field. A hybrid deep architecture has been designed to model local features and global correlations for classifying defects on fabric surfaces. Multi-level features are extracted from input fabric images, and feature maps are adaptively weighted using a channel attention mechanism. The Transformer architecture is used to model long-range global features, thus combining both local and global features. The features transmitted to the classification layer result in highly efficient results. The effectiveness of the method is validated on a 5-class fabric defect dataset, and extensive experiments demonstrate its superior classification performance.

The main contributions of this approach are listed below:

- A hybrid monitoring system combining defect localization and classification has been proposed.
- A learnable fusion mechanism adaptively combining multiple anomaly scores has been developed.
- An explainable deep learning architecture that learns local textural features and global contextual relationships together has been presented.

2. RESEARCH SIGNIFICANCE

This study addresses the need for accurate, explainable, and automated fabric defect inspection in intelligent manufacturing. By integrating transformer-based unsupervised defect localization with CNN-transformer-based supervised classification, the proposed framework enables both precise defect detection and reliable defect recognition within a unified system. The developed approach improves inspection accuracy while providing interpretable visual explanations, making it suitable for real-world quality control applications.

Highlights:

- A unified framework for defect localization and classification is proposed.
- Local texture features and global contextual information are jointly learned.
- Explainable attention maps improve the reliability of defect inspection.

3. LITERATURE REVIEW

Liu et al. [1] proposed a deep learning-based approach for the automatic and reliable detection of industrial fabric defects. The study is based on the fact that complex fabric defect types exist, varying in size and shape. Traditional approaches are insufficient for detecting such defects. The YOLOv4 (You Only Look Once) model, frequently used in object detection, was used to detect small and irregular defects with various improvements. This architecture allows for the rapid identification of the defect location and the classification of common fabric defect types such as holes, oil stains, color defects, and bearing marks. Experimental results show that the proposed method provides approximately a 6% improvement in mean accuracy (mAP) compared to the original YOLOv4 model. However, the processing speed (FPS) of the model decreased by only about 2%, indicating that the system is suitable for real-time applications.

Geze and Akbas [2] performed fabric defect classification on a TILDA dataset with 3200 images in 768×512 dimensions and 12 different defect classes using transfer learning approaches with VGGNet16, InceptionV3, and ResNet50 architectures. After extracting the features of the defective regions in the images using transfer learning architectures, the images were labeled and classified using k-Nearest Neighbor (k-NN) and Support Vector Machine (SVM). They achieved the highest performance with 95.88% accuracy in the ResNet50+k-NN model. Arshad and Shahzad [3], on the other hand, aimed to classify fabric defects by adopting another transfer learning approach. Using ResNet and VGG16Net architectures, they performed one-shot learning on a dataset containing three different fabric defect classes. Each class contains a single instance. This approach aims to provide the model with the ability to label faulty types from a single sample, even for types of faults it hasn't previously encountered. In this context, VGG16Net achieved 73.91% accuracy, while ResNet50 remained at 67.59%.

Varjovi et al. [4] designed a customized deep neural network for classifying fabric faults. This proposed architecture was evaluated on a dataset of 13,800 fabric images with 250x256 pixel values and two classes: faulty and healthy. While the proposed deep model achieved a 97% accuracy rate, among the known transfer learning architectures, InceptionV3, MobileNetV2, and ResNet50, the highest performance on the same dataset was limited to the InceptionV3 architecture with an accuracy rate of 78%. Another study on classifying fabric faults using a transfer learning approach was conducted by Şeker in [5]. In this study, instead of training AlexNet from scratch, pre-trained weights were used. While AlexNet achieved a 75% accuracy rate in training from scratch, it achieved a 98% accuracy rate with AlexNet using pre-trained weights. The dataset used included defects such as tears, knots, oil stains, and double stitching, and consisted of a total of 3725 samples.

To identify defective areas in both plain and printed fabrics, evaluations were made using images from real production environments, specifically Chenab Textiles [6]. The YOLOv8 lightweight model was trained to detect fabric defects. For comparison, the YOLOv5 and Mobilenetv2 SSD FPN lite models were trained on the same dataset. MobilenetSSD-FPNLite achieved the lowest Mean Average Precision (mAP) at 77.09%, followed by YOLOv5 at 84.5%, and YOLOv8 at the highest rate of 84.8%. The dataset used in the study includes seven classes: baekra, color problems, contamination, cuts, gray stitches, edges, and stains.

Revathy and Kalaivani [7] proposed an improved Mask-RCNN model for the detection and classification of defects on the fabric surface. The proposed model includes an innovative solution for small defects and complex background conditions. This model is improved with feature extraction and multi-scale feature merging steps. It aims to classify six different defects, such as holes, stains, transport, yarn defects, line defects, and irregular patterns. Accuracy, mAP, and IoU (Intersection over Union) metrics were used to evaluate the model's performance. In this study, an accuracy rate of 97.8% was achieved. The dataset used contains 50 samples for each class.

Mewada et al. [8] proposed a residual network-based CNN model. Using the ResNet50 architecture as a pre-trained residual network, they achieved 95.36% accuracy in detecting four different fabric defects: holes, objects, oil stains, and yarn defects. In their proposed system, the cuckoo search optimization algorithm was applied in hyperparameter tuning and the fitness function. Liu et al. [9] performed fabric defect detection using an unsupervised UNet network. Mask images were used to identify the defective region. The dataset, created from images obtained from a company in Taiwan, contains 27,000 positive samples and 1,040 negative samples. Training and testing phases were completed on this dataset, and a 69% accuracy rate was obtained from the IoU score. Li et al. [10] designed a hybrid deep model using a channel switching module and a multi-scale coupling module to effectively handle different types of fabric defects and overcome variations in defect sizes. In this study, classification was performed on a dataset containing 7940 samples with twelve different types of defects.

Tastimur et al. [11] achieved classification of four different fabric defects using a Logarithmic Deep Residual Shrinkage network. This specially created dataset was obtained using 2500 image duplication techniques. Experimental results showed an accuracy rate of 99.17%. The proposed model provided approximately a 3% performance gain compared to the classical residual shrinkage network. Tastimur [12] conducted another study for the real-time detection and classification of fabric defects. The proposed model consists of two stages. In the first stage, segmentation was applied to defective regions in fabric images using Fuzzy C-means, Conditional Random Fields (CRF), and U-Net enhanced with spatial attention. Then, the dataset used consisted of 2555 fabric images clustered into two groups: defective and healthy. The accuracy obtained was 99.92%.

Islam et al. [13] classified fabric defects using a hybrid approach based on community learning and deep learning. Training was conducted on a dataset consisting of six specially created defects (broken-button, button-hike, color-defect, foreign-yarn, hole, and sewing-error). Defect detection was applied using the YOLOv8m architecture, and the mAP@50 value was measured as 89%. In the classification phase, five different transfer learning architectures—VGG16, ResNet50, MobileNet, InceptionV3, and Xception—were used, and the outputs of these architectures were combined using a weighted voting method. Experimental studies showed a 90% accuracy rate.

Table 1. Studies in the literature on steel defect detection and diagnosis

Refs.	Method Used	Dataset	Metric
[2]	VGG16, InceptionV3, ResNet50 + k-NN, SVM	TILDA, 3,200 images, 12 classes	95.88% (ResNet50 + k-NN)
[3]	VGG16, ResNet50 (One-shot learning)	3 classes (single-sample setting)	73.91% (VGG16), 67.59% (ResNet50)
[4]	Custom CNN model	13,800 images, 2 classes	97% accuracy
[5]	Transfer learning with AlexNet	3,725 images, multi-class	98% (pre-trained)
[6]	YOLOv8, YOLOv5, MobileNetSSD	7 classes	84.8% (YOLOv8), 84.5% (YOLOv5), 77.09%
[7]	Improved Mask R-CNN	6 classes, 50 samples per class	97.8% accuracy
[8]	ResNet50 + Cuckoo Search	4 classes	95.36% accuracy
[9]	Unsupervised U-Net (segmentation)	27,000 positive, 1,040 negative samples	IoU: 69%
[11]	Log Deep Residual Shrinkage	2,500 images, 4 classes	99.17% accuracy
[12]	U-Net + FCM + CRF + Attention	2,555 images, 2 classes	99.92% accuracy
[13]	YOLOv8 + Ensemble CNN	6 classes	mAP: 89%, Accuracy: 90%
[14]	EfficientNet, ResNet, RegNet + Adam/Ranger	8,073 images, 5 classes	99.42% accuracy
[15]	Transfer learning + sliding window	5 different datasets	98.62% accuracy
[17]	Simple CNN	Binary classification	~80% accuracy

Guder et al. [14] created a custom dataset by combining the TILDA and Wiever datasets for classifying defects on fabric surfaces. The resulting dataset consists of 8073 images with a resolution of 256×256 pixels, each containing five different defects: line defects, wrinkle marks, machine oil stains, holes, and bleaching defects. Classification was performed using different transfer learning approaches, such as EfficientNetB4, EfficientNetV2M, ResNet18, and RegNetZ_E8, and the results were compared. In addition, the optimizer algorithm was tested with different versions (Adam and Ranger). The highest performance was achieved with Adam + EfficientNetv2m, reaching an accuracy rate of 99.42%.

Jing et al. [15], who performed fabric defect classification using transfer learning architectures, used five different fabric datasets comparatively in the training and testing phases. In the proposed approach, the best initial parameters were recorded using pre-weights previously trained with the MNIST dataset. Then, the input image was divided into local regions, and these regions and weight coefficients were fine-tuned to the trained model. Defective areas and defect types were then detected using the sliding window method. The success rate achieved by the proposed model increased by approximately 9% compared to the pre-trained weighted model training, reaching a peak of 98.62%. In this study, which proposes the real-time and automatic detection of fabric defects, the YOLOv11 model was adopted in [16]. The proposed architecture was tested on white and linen fabrics for defects such as holes, discoloration, and wrinkles. Experiments were conducted in a real industrial environment under controlled lighting and with two RealSense cameras placed approximately 1 meter away from the fabric. The results show that the system offers high accuracy and low latency with an mAP@0.5 value of over 82%. Ananthi et al. [17] used a binary classification system for fabric surface defect classification, labeling them as healthy/defective. The dataset examples used included defects such as holes, missing threads, and minor irregularities. In this study, an accuracy rate of approximately 80% was achieved using a simple CNN network.

4. THE PROPOSED APPROACH

The proposed architecture consists of two components: unsupervised anomaly detection and supervised anomaly classification. In the first stage, the input image is divided into $I \in \mathbb{R}^{H \times W \times C}$ P×P-sized patches to detect anomaly regions unsupervised. The total number of patches obtained in the image is $N = \frac{H \times W}{P^2}$. Local patterns in the image are transferred to lower and more regular feature representations. The patch embeddings are passed through a convolutional projection to obtain the representation vector in (1). Here, X_i represents the input patch; W_p represents the learnable projection weights; b_p represents the bias term; and Z_i represents the obtained embedding vector. Thanks to self-attention in the transformer architecture, long-range relationships in the input images are modeled as in (2) through the query, value, and key matrices. Here, Q, K, and V represent the query, key, and value matrices, respectively, and d_k represents the scaling factor. The outputs from the transformer encoder layer were used in the anomaly locus test.

$$Z_i = W_P X_i + b_P \quad (1)$$

$$Attention(Q, K, V) = Softmax\left(\frac{QK^T}{\sqrt{d_k}}\right)V \quad (2)$$

In this study, data distribution is learned only from healthy fabric data in the detection of anomaly regions. After normalization with the generated patch feature matrices (3), they are stored in the memory bank. Here, x represents the feature vector and $\hat{x}$ represents the normalized representation vector. The memory structure contains only the representations of normal samples, and a similarity-based anomaly score is generated in the test phase. The anomaly score is obtained as follows: first, the test image is passed through the transformer block to obtain patch embedding, then the distance between the features in the memory bank is calculated with Euclidean (4), and the anomaly score is obtained through the nearest neighbor similarity. Scores obtained by deviating from the normal distribution indicate the presence of an anomaly region. In addition, it is not limited to only similarity-based measurement, but the Mahalanobis distance is also used to model statistical distribution deviations. By learning the mean and covariance structure of the features obtained from normal samples, the extent to which the test features deviate from the distribution is calculated.

$$\hat{x} = \frac{x}{\|x\|_2} \tag{3}$$

$$d(x, m_i) = \|x - m_i\|_2 \tag{4}$$

Here, m_i represents the reference feature in the memory bank. For each patch, the mean distance of the nearest neighbor is calculated to obtain the similarity-based anomaly score (5). In the proposed method, in addition to similarity-based anomaly analysis, Mahalanobis distance is used for statistical distribution modeling. First, the mean vector of features obtained from healthy samples is calculated in (6) and (7), the covariance matrix and Mahalanobis distance in (8). This enables the model to detect regions that deviate from normal feature representations as defects. Mahalanobis distance provides important supplementary information, especially for low-contrast defects and complex surface structures.

$$S_{mem}(x) = \frac{1}{k}\sum_{i=1}^{k} d(x, m_i) \tag{5}$$

$$\mu = \frac{1}{N}\sum_{i=1}^{N} m_i \tag{6}$$

$$\Sigma = \frac{1}{N-1}\sum_{i=1}^{N}(x_i - \mu)(x_i - \mu)^T \tag{7}$$

$$D_M(x) = \sqrt{(x - \mu)^T \Sigma (x - \mu)^{-1}} \tag{8}$$

$$w_i = \frac{e^{\alpha_i}}{\sum_{j=1}^{n} e^{\alpha_j}} \tag{9}$$

$$S_{final} = w_1 S_{trans} + w_2 S_{mem} + w_3 S_{mah} \tag{10}$$

Focusing on anomaly regions is ensured by using the representation deviation score calculated in the transformer encoder output and the statistical distribution differences. These two representation scores are combined with the adaptive fusion in (9). Here, α_i represents the learnable parameters, and w_i represents the normalized weights. The final anomaly score (10) is also obtained. Here, S_{trans} represents the Transformer representation deviation; S_{mem} represents the memory bank distance; and S_{mah} represents the Mahalanobis score. Thanks to this adaptive fusion strategy, the complementary features of different anomaly criteria are optimized, and more stable anomaly maps are obtained. Afterwards, the anomaly scores are normalized and rescaled to the image size.

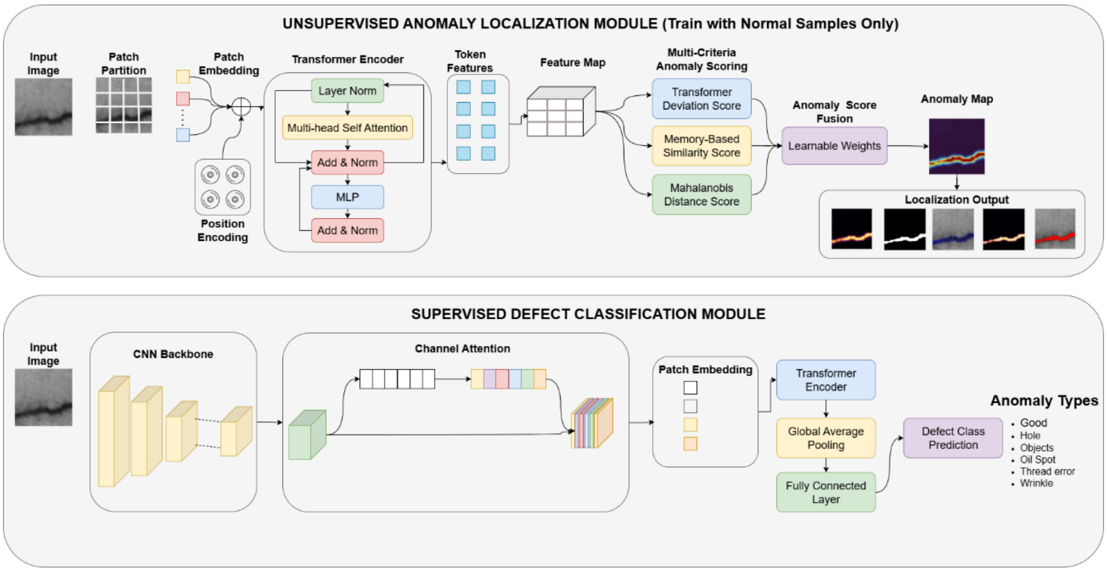

Figure 1. The overview of the proposed model for KAN-based steel surface defect diagnosis

5. EXPERIMENTAL RESULTS

Several experimental studies have been conducted to evaluate the performance of the proposed model. The experimental studies used sample images of defective fabric from our defect dataset, consisting of four different surface defects, as shown in Figure 3. Detailed performance analyses were presented with the proposed model with common hyperparameter tuning. The hyperparameter tuning used in the study was as follows: AdamW was used as the optimizer algorithm during training, with an initial learning rate of 0.0001, batch size of 32, an epoch of 50, and a 0.3 dropout between layers to prevent overfitting.

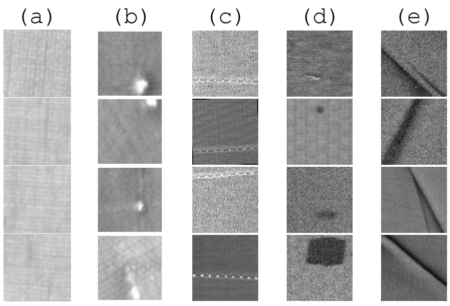

Figure 3. Examples from our fabric defect dataset. a)good, b)hole, c)horizontal, d)stain, e)wrinkle

5.1. Performance Analysis of the Proposed Model

To ensure a fair evaluation of the classical CNN model with the proposed model, all layers and hyperparameter adjustments were used on the same dataset. The classification performance of the proposed model is presented comparatively with accuracy, precision, recall, and F1 score values in tables and trend graphs. Figure 4 shows the accuracy curves, recall, precision, and F1 scores comparatively. As can be seen in Table 2, the test accuracy of the proposed model is 97.78%. The confusion matrices in Figure 5 reveal that the proposed model had 30 false positives. Based on these performances, Receiver Operating Characteristic (ROC) curve and Area Under the Curve (AUC) analyses were performed to examine the classification reliability of the model at different decision thresholds. The obtained ROC curves, shown in Figure

6, demonstrate that the proposed model produces higher true positive rates and lower false positive rate values.

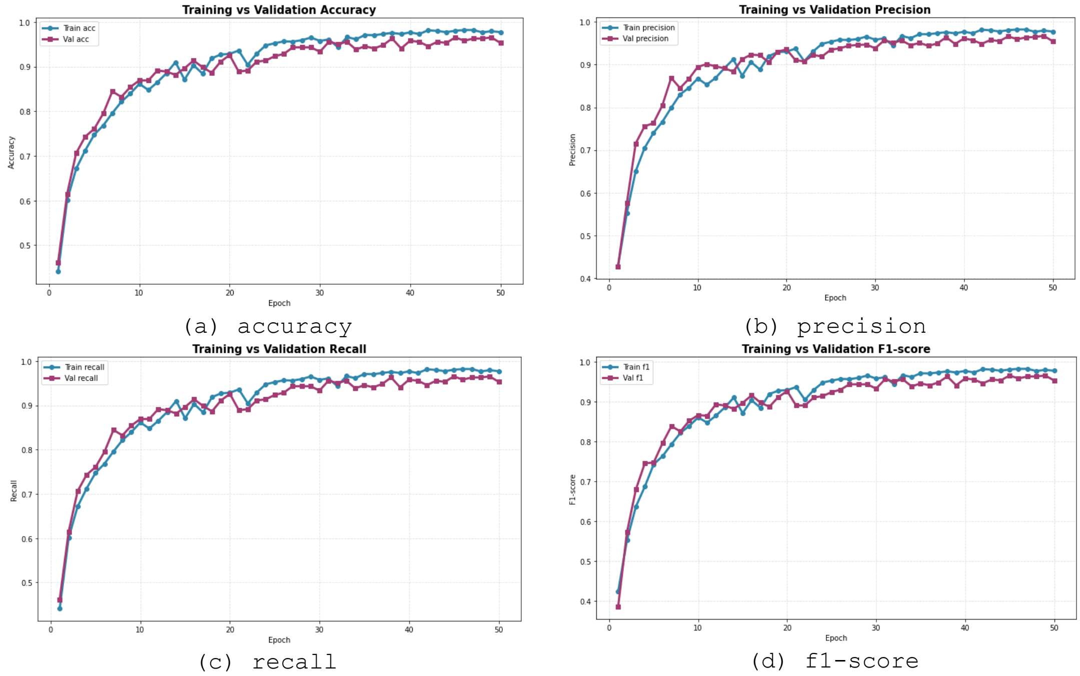

(a) accuracy (b) precision

(c) recall (d) f1-score

Figure 4. Accuracy, precision, recall, and f1-score curves during training and validation for the proposed model

Table 2. Classification performance of our model

Metrics	Training	Validation	Testing
Accuracy	0.9772	0.9531	0.9778
Precision	0.9773	0.9548	0.9779
Recall	0.9772	0.9531	0.9778
F1-Score	0.9773	0.9530	0.9778

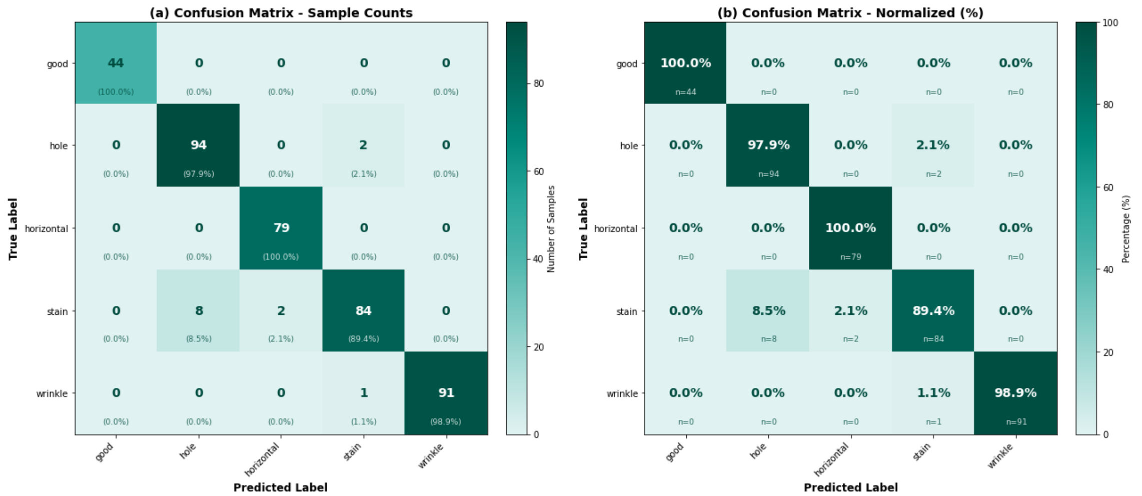

Figure 5. Confusion Matrice of our model

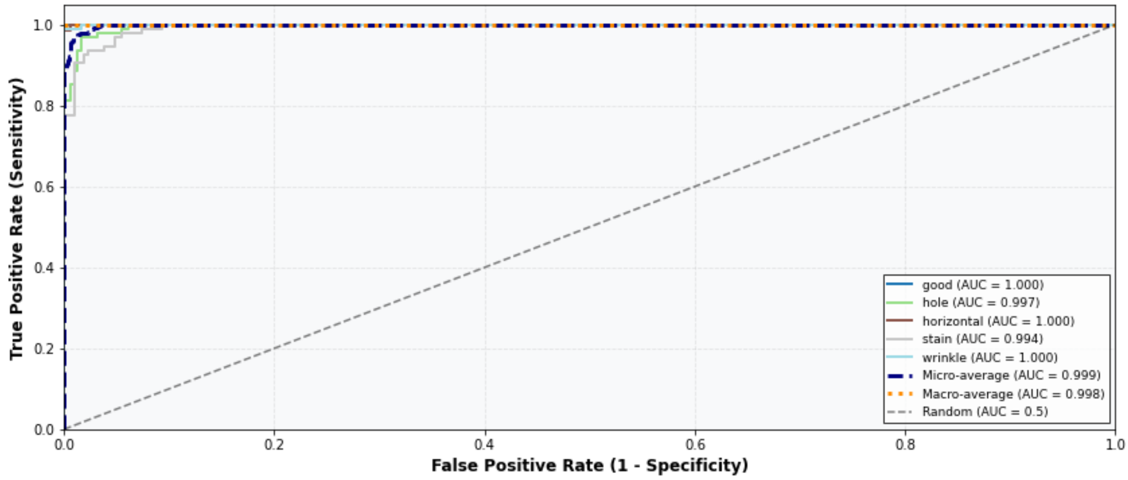

Figure 6. ROC curve of our model

Table 3. Per-class classification results of the proposed model

Classes	P	R	F1	Support
Good	1.0000	1.0000	1.0000	44
Hole	0.9216	0.9792	0.9495	96
Horizontal	0.9753	1.0000	0.9875	79
Stain	0.9655	0.8936	0.9282	94
Wrinkle	1.0000	0.9891	0.9945	92

The comparative results of the proposed model in terms of precision, recall, and F1 score values among the fault types classified are presented in Table 3. When these metrics are examined, our model is superior in terms of inter-class discrimination power. To analyze the learned representations in the feature space, dimensionality reduction visualizations based on UMAP in Figure 7. The visualization results show that the proposed model groups samples belonging to the same class into more compact clusters and makes the inter-class discrimination more pronounced.

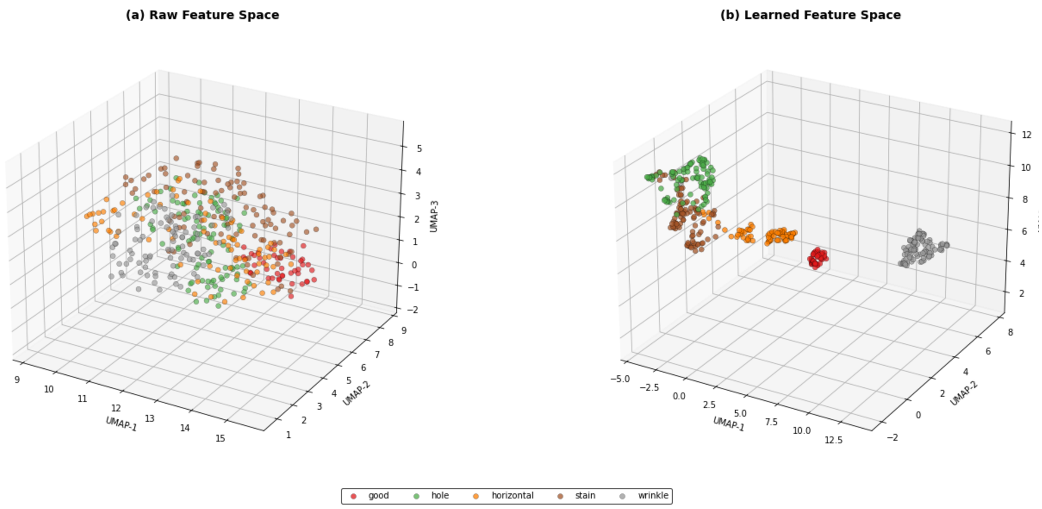

Figure 7. UMAP visualization of the proposed model

5.2. Visual Interpretability and Defect Localization Analysis

To better analyze the localization capability and decision-making behavior of the proposed framework, several visualization and interpretability strategies were integrated into the defect inspection pipeline.

Table 4. Visual interpretation of the proposed defect detection framework across processing stages

Original	Inferno Heatmap	Turbo Heatmap	Binary Mask	Contour	Overlay	Fusion Output

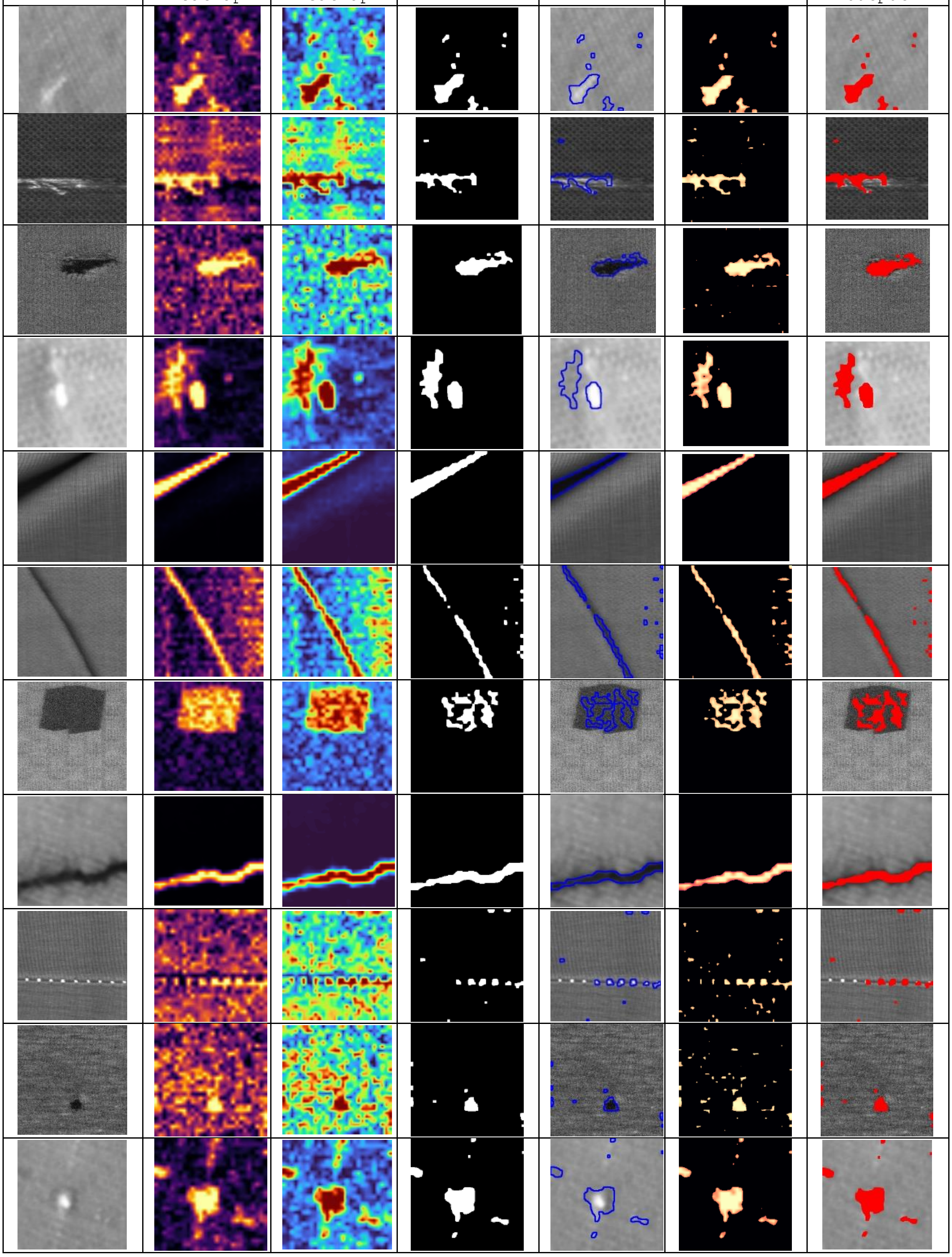

The proposed method generates multiple anomaly-aware visualization outputs, including normalized anomaly heatmaps, adaptive binary localization masks, contour-based defect boundaries, transparent anomaly overlays, and edge-enhanced defect representations. As illustrated in Table 4, the visualization framework consists of the original input image, anomaly heatmaps generated from the adaptive anomaly fusion module, threshold-based binary masks, contour localization outputs, transparent overlay maps, and the final fused defect visualization results. The anomaly localization process is driven by the proposed adaptive multi-criteria anomaly analysis strategy, which combines Transformer-based feature deviations, memory-guided similarity responses, and Mahalanobis statistical distance measurements.

The generated anomaly activation maps represent deviations from the learned normal feature distribution and highlight spatial regions associated with potential surface defects. Higher activation intensities indicate stronger anomaly confidence scores produced by the fusion mechanism. Different colormap representations, including Inferno, Turbo, and Magma-based heatmaps, are utilized to improve the visual discrimination of anomalous regions and enhance localization interpretability. To obtain more spatially consistent localization results, adaptive thresholding and morphological refinement operations are applied to the anomaly maps. Binary defect masks are generated using statistical threshold estimation based on the anomaly score distribution, while morphological opening and closing operations suppress noise and improve structural continuity. In addition, contour extraction is employed to explicitly visualize defect boundaries and emphasize geometric irregularities on the surface. Edge-enhanced representations obtained through gradient-based extraction further improve the visibility of fine defect structures and boundary transitions.

Finally, the proposed fusion visualization strategy integrates anomaly heatmaps, contour information, transparent overlays, and edge-enhanced representations to generate a comprehensive and explainable defect localization output. By combining complementary spatial and statistical information from different feature representations, the proposed visualization pipeline provides more robust interpretability and more accurate delineation of defect regions. These visualization results demonstrate that the proposed framework is capable of effectively highlighting defect-sensitive regions while preserving the structural characteristics of industrial surface textures.

6. CONCLUSIONS

In this study, a hybrid and explainable deep learning framework was proposed for industrial defect localization and classification. The proposed system combines contextual anomaly localization, adaptive anomaly fusion, and hybrid feature learning within a unified inspection architecture. Transformer-based contextual representation learning, memory-guided anomaly analysis, and statistical deviation modeling were jointly utilized to improve localization sensitivity, while the classification module effectively captured both local texture patterns and global spatial dependencies. In addition, multiple visualization strategies, including anomaly heatmaps, contour localization, and transparent overlays, enhanced the interpretability of the proposed framework. Experimental results demonstrated that the proposed method achieved strong defect localization capability and high classification performance on complex industrial surface defects. The adaptive fusion strategy and hybrid representation learning approach provided more robust and spatially consistent inspection results compared to conventional methods. Compared with existing industrial inspection approaches, the proposed framework offers superior robustness against complex defect patterns by effectively integrating anomaly localization and discriminative feature learning within a single architecture. Furthermore, its explainable visualization mechanism improves the transparency and reliability of inspection results, while the adaptive fusion strategy enables more accurate and consistent defect localization and classification across different defect categories. For future work, lightweight model optimization for real-time industrial applications, self-supervised learning strategies, and multimodal inspection approaches may be investigated. In addition, advanced contextual modeling techniques and foundation-based architecture could further improve anomaly understanding and generalization performance in industrial quality inspection systems.

CONFLICT OF INTEREST

The authors declared that they have no potential conflict of interest.

FINANCIAL DISCLOSURE

This research received no financial support.

DECLARATION OF ETHICAL STANDARDS

The authors of the article declare that the materials and methods used did not require ethics committee approval and/or regulatory approval.

REFERENCES

[1] Liu, Q., Wang, C., Li, Y., Gao, M., and Li, J., (2022). A fabric defect detection method based on deep learning. IEEE Access, 10, 4284-4296.

[2] Geze, R.A. and Akbaş, A., (2024). Detection and classification of fabric defects using deep learning algorithms, Journal of Polytechnic, 27(1):371-378.

[3] Arshad, S.R. and Shahzad, M.K., (2024). Deep learning-based fabric defect detection. Research Reports on Computer Science, 1-11.

[4] Varjovi, M.H., Talu, M.F., and Hanbay, K., (2022). Fabric defect detection using customized deep convolutional neural network for circular knitting fabrics. Türk Doğa ve Fen Dergisi, 11(3):160-165.

[5] Şeker, A., (2018). Evaluation of fabric defect detection based on transfer learning with pre-trained AlexNet. In 2018 International conference on artificial intelligence and data processing (IDAP) (pp:1-4). IEEE.

[6] Nasim, M., Mumtaz, R., Ahmad, M., and Ali, A., (2024). Fabric Defect Detection in Real World Manufacturing Using Deep Learning. Information, 15(8):476.

[7] Revathy, G. and Kalaivani, R., (2024). Fabric defect detection and classification via deep learning-based improved Mask RCNN. Signal, Image and Video Processing, 18(3):2183-2193.

[8] Mewada, H., Pires, I.M., Engineer, P., and Patel, A.V., (2024). Fabric surface defect classification and systematic analysis using a cuckoo search optimized deep residual network. Engineering Science and Technology, an International Journal, 53, 101681.

[9] Liu, K.H., Chen, S.J., and Liu, T.J., (2022). Unsupervised unet for fabric defect detection. In 2022 IEEE International Conference on Consumer Electronics-Taiwan (pp. 205-206). IEEE.

[10] Li, S., Sun, W., Liang, Q., Sun, J., and Liu, C., (2024). Multimodal fabric defect classification using channel switching and multiscale feature fusion. IEEE Transactions on Instrumentation and Measurement, 74:1-12.

[11] Tastimur, C., Akin, E., and Agrikli, M., (2025). Fabric Faults Robust Classification Based on Logarithmic Residual Shrinkage Network in a Four-Point System. Applied Sciences, 15(12):6783. https://doi.org/10.3390/app15126783

[12] Tastimur, C., (2026). Automated fabric defect inspection with fuzzy c-means, conditional random fields and refined U-Net. J Mech Sci Technol, 40:597–607. https://doi.org/10.1007/s12206-025-1250-x
[13] Islam, R., Ullah, S., Rahaman, S., Sheebly, J., Rahman, S., and Rahman, R., (2024). ensemble deep learning for real-time textile fabric defect detection and classification using YOLOv8 and CNNs. In Proceedings of the 3rd International Conference on Computing Advancements (pp:939-945).
[14] Guder, O., Isik, S., and Anagun, Y., (2025). Fabric defects identification for textile industry with a deep learning approach. The Journal of The Textile Institute, 116(8):1493–1502. https://doi.org/10.1080/00405000.2024.2383799
[15] Jing, J.F., Ma, H., and Zhang, H.H., (2019). Automatic fabric defect detection using a deep convolutional neural network. Coloration Technology, 135(3):213-223.
[16] Machado, R., Barros, L.A.M., Vieira, V., Silva, F.D.D., Costa, H., and Carvalho, V., (2025). Textile Defect Detection Using Artificial Intelligence and Computer Vision—A Preliminary Deep Learning Approach. Electronics, 14(18):3692.
[17] Ananthi, S., Preetha, R., Soundharya, S., Swathi, S., and Vanitha, M.V., (2024). Smart Fabric Inspector System using Deep Learning Algorithm. In 2024 3rd International Conference on Automation, Computing and Renewable Systems (ICACRS) (pp. 1493-1500). IEEE.